Glenney, J. (1986) *J. Biol. Chem. 261*, 7247.
Glenney, J. R., Tack, B., & Powell, M. A. (1987) *J. Cell Biol. 104*, 503.
Grykiewics, G., Poenie, M., & Tsien, R. Y. (1985) *J. Biol. Chem. 260*, 3440.
Hope, M. J., Bally, M. B., Webb, G., & Cullis, P. R. (1985) *Biochim. Biophys. Acta 812*, 55.
Huang, C. (1969) *Biochemistry 8*, 344.
Hummel, J. P., & Dreyer, W. J. (1962) *Biochim. Biophys. Acta 63*, 530.
Khanna, N. C., Helwig, E. D., Ikebuchi, N. W., Fitzpatrick, S., Bajwa, R., & Waisman, D. M. (1990) *Biochemistry 29*, 4852.
Klee, C. B. (1988) *Biochemistry 27*, 6645.
Klee, C. B., Crouch, T. H., & Richman, P. G. (1980) *Annu. Rev. Biochem. 49*, 489.
Kretsinger, R. H. (1976) *Annu. Rev. Biochem. 45*, 239.
Kretsinger, R. H. (1980) *CRC Crit. Rev. Biochem. 8*, 119.
Laemmli, M. K. (1970) *Nature (London) 227*, 680.
Nelsestuen, G. L. (1988) in *Current Advances in Vitamin K Research* (Suttie, J. W., Ed.) p 335, Elsevier, New York.
Nelsestuen, G. L., & Lim, T. K. (1977) *Biochemistry 16*, 4164.
Ohno, S., Kawasaki, H., Imajoh, S., Suzuki, K., Inagaki, M., Yokokura, H., Sakoh, T., & Hidaka, H. (1987) *Nature (London) 325*, 161.
Owens, R. J., & Crumpton, M. J. (1984) *Biochem. J. 219*, 309.
Parker, P. J., Stabel, S., & Waterfield, M. D. (1984) *EMBO J. 3*, 953.
Parker, P. J., Coussens, L., Totty, N., Rhee, L., Young, S., Chen, E., Stabel, S., Waterfield, M. D., & Ullrich, A. (1986) *Science (Washington, D.C.) 233*, 853.
Portis, A., Newton, C., Pangborn, W., & Papahadjopoulos, D. (1979) *Biochemistry 18*, 780.
Schlaepfer, D. D., & Haigler, H. T. (1987) *J. Biol. Chem. 262*, 6931.
Schwalbe, R. A., Ryan, J., Stern, D. M., Kisie, W., Dahlbäck, B., & Nelsestuen, G. L. (1989) *J. Biol. Chem. 264*, 20288.
Shadle, P. J., Gerke, V., & Weber, K. (1985) *J. Biol. Chem. 260*, 16354.
Sommerville, L. E., Resnick, R. M., Thomas, D. D., & Nelsestuen, G. L. (1986) *J. Biol. Chem. 261*, 6222.
Weber, K., Johnson, N., Plessmann, U., Van, P. N., Söling, H.-D., Ampe, C., & Vandekerckhove, J. (1987) *EMBO J. 6*, 1599.

Serpin–Serine Protease Binding Kinetics: α_2-Antiplasmin as a Model Inhibitor

Colin Longstaff* and Patrick J. Gaffney
National Institute for Biological Standards and Control, Blanche Lane, South Mimms, Herts EN6 3QG, U.K.
Received May 8, 1990; Revised Manuscript Received October 5, 1990

ABSTRACT: We have examined in detail the kinetics of binding of the serpin α_2-antiplasmin to the serine proteases α-chymotrypsin and plasmin. These represent model systems for serpin binding. We find, in contrast to earlier published results with α_2-antiplasmin and plasmin, that binding is reversible, and slow binding kinetics can be observed, under appropriate conditions. Binding follows a two-step process with both enzymes, with the formation of an initial loose complex which then proceeds to a tightly bound complex. In the absence of lysine and analogues, equilibrium between α_2-antiplasmin and plasmin is achieved rapidly, with an overall inhibition constant (K_i') of 0.3 pM. In the presence of tranexamic acid or 6-aminohexanoic acid, lysine analogues that mimic the effects of fibrin, plasmin binding kinetics are changed such that equilibrium is reached slowly following a lag phase after mixing of enzyme and inhibitor. The K_i' is also affected, rising to 2 pM in the presence of 6-aminohexanoic acid concentrations above 15 mM. Thus extrapolation to the in vivo situation indicates that complex formation in the presence of fibrin will be delayed, allowing a burst of enzyme activity following plasmin generation, but a tight, pseudoirreversible complex will result eventually. Chymotrypsin is more weakly inhibited by α_2-antiplasmin, exhibiting an overall K_i' of 0.1 nM, after two-stage complex formation. The inhibition constant for the initial loose complex (K_i) is very similar for both enzymes. The difference in binding strength between the two enzymes is accounted for by the dissociation rate constant of the second step of complex formation. To our knowledge, this rate constant has previously not been measured for serpin interactions. The reversibility of binding argues against a complex having a covalent bond between enzyme and inhibitor. This mechanism of binding has important consequences for the measurement of serpin activity. Structure/function relationships are discussed to explain inhibitory action.

Control of serine protease activity is central to the biochemistry of blood clotting and of fibrinolysis. Unwanted proteolytic activity is prevented by the production of zymogens and, following activation, by inhibition with protein inhibitors. Serpins are a family of serine protease inhibitors present at key points in clotting and fibrinolytic pathways. Although serpins have been the subject of much research in recent years [e.g., see Huber and Carrell (1989)], there is still no generally accepted mechanism explaining how these proteins are able to act as protease inhibitors. To begin to address this question, it is necessary to carry out functional studies including kinetic analysis of binding. More complete understanding will come with detailed X-ray crystal structures of serpin complexes, but this is unavailable at present. Serpins are known to form stable 1:1 complexes with serine proteases, but the factors responsible for ensuring that the bound protein is not hydrolyzed are poorly understood. We have used the serpin α_2-antiplasmin to investigate the kinetics of inhibitor binding with two enzymes,

0006-2960/91/0430-979$02.50/0

plasmin and chymotrypsin. Plasmin is the enzyme responsible for digesting fibrin and is the target enzyme for α_2-antiplasmin (Collen et al., 1976; Moroi & Aoki, 1976; Mullertz & Clemensen, 1976); chymotrypsin is used here as a model serine protease with this inhibitor.

The earliest studies on α_2-antiplasmin binding to plasmin led to a mechanism for binding as shown in scheme I (Wiman & Collen, 1978; Wiman et al., 1978). This has also been proposed as a general model for serpin binding to serine proteases (Travis & Salvesen, 1983). Scheme I shows the reversible formation of an initial loose complex, EI, followed by the irreversible formation of complex EI'. On the basis of the observed value of k_2, and by analogy with other small protein protease inhibitors for which crystal structures were available, for example, bovine pancreatic trypsin inhibitor (Rühlmann et al., 1973), it was proposed that this second step represented covalent bond formation (Travis & Salvesen, 1983).

Scheme I

$$\text{enzyme} + \text{inhibitor} \underset{k_{-1}}{\overset{k_1}{\rightleftharpoons}} \text{EI} \xrightarrow{k_2} \text{EI}'$$

A great deal of kinetic work has been done on serine protease–protein inhibitor binding (e.g., of the Kunitz, ovomucoid types, etc.), which shows complex formation follows a series of reversible steps (Laskowski & Kato, 1980). There are some reports in the literature that intact serpin can be recovered from complexes, i.e., that complex formation can be reversed under some circumstances (Ohlsson & Laurell, 1976; Shieh et al., 1989). Specifically, the recent work of Shieh et al. demonstrates that trypsin or chymotrypsin could be displaced from complexes with α_2-antiplasmin by α_2-macroglobulin. The released α_2-antiplasmin was not cleaved, indicating a reversible component to complex formation. In light of these and other observations it seemed worthwhile to look again at serpin binding to see if this family does indeed have a different mechanism of binding than small protease inhibitors. Alternatively, the original proposals for serpin binding may need modification. We have used a slow binding kinetics approach to look at this system [for reviews on slow binding kinetics see Cha (1975) and Morrison and Walsh (1988)]. This has recently been applied successfully to another serine protease–small protein inhibitor system (Longstaff et al., 1990). The results from these studies will have implications for serpin–protease systems in general.

Materials and Methods

Purified α_2-antiplasmin was a gift from Dr. H. R. Lijnen, University of Leuven, Belgium. Protein was supplied as a lyophilized powder which was reconstituted in distilled water to a stock solution, which was flash frozen in aliquots and stored at −40 °C before use. The concentration of active inhibitor was determined by titration against purified plasmin of known concentration (see below).

Human Lys-plasminogen was a gift provided by Professor A. Sasahara of Abbott Laboratories, Chicago. This plasminogen was a mixture of two zymogen forms, types I and II, known to have different carbohydrate compositions and different affinities for substrates and inhibitors (Lijnen et al., 1981). Further purification was carried out to separate type I and type II plasminogens, essentially following the chromatographic procedure of Nieuwenhuizen and Traas (1989), using a lysine–Sepharose column made by coupling lysine to cyanogen bromide activated Sepharose (Pharmacia), as previously described (Deutch & Mertz, 1970). Plasminogen type II (the second eluting peak) was used in these studies and was activated to plasmin by use of immobilized urokinase (a gift from Serrono Laboratories, Rome). Urokinase was coupled to cyanogen bromide activated Sepharose to a concentration of 1 mg/mL in 0.1 M sodium borate buffer, pH 8.6, containing 0.5 M sodium chloride, according to the manufacturer's instructions. Maximum activation of plasminogen occurred after 20-min incubation at 25 °C using 50 μL of gel to 1 mL of plasminogen solution. Plasmin activity was stable for several hours under these conditions. Active plasmin was flash frozen and stored in aliquots at −40 °C for future use. No loss of activity was noted over a period of 6 months. Purity of plasmin(ogen) pools was checked by SDS–PAGE (see below).

Concentration of Active Sites. Plasmin active site titrations were performed with 4-methylumbelliferyl *p*-guanidinobenzoate hydrochloride (MUGB)[1] (Sigma Chemical Co.), essentially as described by Jameson et al. (1973). Stock MUGB solutions were made up freshly by dissolving approximately 5 mg in 1 mL of *N*-methylpyrrolidinone. This was then diluted with 1 mM HCl to give a working solution of 1 mM titrant. An aliquot (2 μL) was then added to 2 mL of PBS, followed by 15–50 μL of enzyme solution. The increase in relative fluorescence with time was monitored (excitation 325 nm; emission 445 nm) until a steady-state turnover rate was observed. Urokinase, M_r 55 000 (a gift from Wakomoto, Japan), and trypsin (Sigma Chemical Co.) were titrated similarly. α-Chymotrypsin (Sigma Chemical Co.) was titrated by using 4-methylumbelliferyl *p*-(*N*,*N*,*N*-trimethylammonio)cinnamate (MUTMAC) (Sigma Chemical Co.) (Jameson et al., 1973). Standard curves were made for both titrants by using 4-methylumbelliferone in PBS.

Catalytic constants for plasmin were determined in 0.1 M Tris-HCl buffer, pH 7.4, containing 0.01% Tween 80, at 25 °C, with the substrate S-2251 (Val-Leu-Lys-*p*-nitroanilide, Kabi Diagnostics, Sweden). Under these conditions K_m = 0.2 mM and k_{cat} = 28 s^{-1}. α-Chymotrypsin was assayed in 0.144 M Tris-HCl buffer, pH 7.78, containing 0.01% Tween 80, at 25 °C, with the substrate succinyl-Ala-Ala-Pro-Phe-*p*-nitroanilide (Sigma Chemical Co.). K_m and k_{cat} were determined to be 0.045 mM and 43 s^{-1}, respectively.

The same buffers were used in the inhibition kinetics experiments described below. Trypsin assays were performed in 0.1 M Tris-HCl buffer, pH 8.0, containing 0.01% Tween 80, with the chromogenic substrate benzoyl-L-arginine-*p*-nitroanilide (Sigma Chemical Co.). Urokinase assays were performed in 0.1 M Tris-HCl buffer, pH 8.8, containing 0.01% Tween 80, with the chromogenic substrate S-2244 (pyroglutamyl-Gly-Arg-*p*-nitroanilide, Kabi Diagnostics, Sweden).

Inhibition Progress Binding Curves. To determine association rate constants, dissociation rate constants, and inhibition constants for α_2-antiplasmin–serine protease interactions, the onset of inhibition was monitored by adding enzyme solution to a mixture of chromogenic substrate and inhibitor. In some cases (see Results), effector was also present, either tranexamic acid [*trans*-4-(aminomethyl)cyclohexanecarboxylic acid] or 6-aminohexanoic acid (both Sigma Chemical Co.). These molecules are known to slow down the rate of reaction of plasmin and α_2-antiplasmin. For experiments with plasmin, concentrations were 0.5 nM enzyme, 1 mM substrate (S-

[1] Abbreviations: SDS–PAGE, sodium dodecyl sulfate–polyacrylamide electrophoresis; PBS, phosphate-buffered saline; MUGB, 4-methylumbelliferyl *p*-guanidinobenzoate hydrochloride; MUTMAC, 4-methylumbelliferyl *p*-(*N*,*N*,*N*-trimethylammonio)cinnamate; S-2251, Val-Leu-Lys-*p*-nitroanilide; S-2444, pyroglutamyl-Gly-Arg-*p*-nitroanilide; SD, standard deviation; BPTI, bovine pancreatic trypsin inhibitor; t-PA, tissue plasminogen activator; PAI-1, plasminogen activator inhibitor 1. P_i notation is from Schecter and Berger (1967).

2251), 2.5–13 nM α_2-antiplasmin, and 5–500 μM tranexamic acid or 15–50 mM 6-aminohexanoic acid (see Results). Data were collected for 10 h in order to establish good estimates for final steady-state rates. Corrections were made for nonenzymatic substrate hydrolysis where necessary.

Chymotrypsin–α_2-antiplasmin binding kinetics were studied similarly by using 0.4 mM substrate (succinyl-Ala-Ala-Pro-Phe-*p*-nitroanilide), 0.4 nM enzyme, and 5–40 nM inhibitor. Reactions were monitored for up to 5 h.

Inhibitor binding was monitored essentially as described by Longstaff et al. (1990). Briefly, enzyme solution (100 μL) was added to 0.9 mL of solution in a cuvette at 25 °C containing buffer, chromogenic substrate, inhibitor, and effector (where present; see Results). The solution was mixed and placed in a DU-6 spectrophotometer fitted with a six-cell transport mechanism. In this way data from six progress curves were collected simultaneously.

Data were fitted to the integrated rate equation for slow binding inhibition (eq 1) [e.g., see Morrison and Walsh (1988)], by nonlinear regression analysis using Enzfitter (Leatherbarrow, 1987). Fitting generated values for v_0 (initial rate), v_s (final steady-state rate), k' (apparent rate constant for the transition from v_0 to v_s), and A_0 (the initial absorbance at 405 nm), for each of the binding curves. These values were then treated in various ways to generate rate constants and inhibition constants (see Results). In addition, a value for v_i (enzyme reaction rate in the absence of inhibitor) was established for each experiment. In all determinations, less than 5% of the chromogenic substrate was used before the completion of the experiment.

$$A = v_s t + (v_0 - v_s)(1 - e^{-k't})/k' + A_0 \qquad (1)$$

Dissociation of Preformed Complexes. Complex of chymotrypsin and α_2-antiplasmin was made by mixing 5 μM enzyme (10 μL) with 7.2 μM inhibitor (10 μL) and incubating for 1 h on ice. This was then quickly diluted 10^4-fold into 0.9 mM substrate (1 mL) in buffer and dissociation of free enzyme observed with time (absorbance at 405 nm) at 25 °C. A cuvette containing 0.25 nM enzyme alone was monitored simultaneously to give the maximum rate for dissociated complex. Depletion of substrate had no significant effect on enzyme rate over the time course of these experiments. Data points collected over 5 h, at 1-min intervals, were fitted to eq 2 by nonlinear regression analysis using Enzfitter (Leatherbarrow, 1987). k_{off} is the dissociation rate constant for the dissociation of complex [i.e., k_{off} or k_{-2} according to mechanism A or B, Scheme II (Results), respectively].

$$A = \frac{k_{cat}[E_0][S](k_{off} + e^{-k_{off}t} - 1)}{k_{off}K_m[S]} + A_0 \qquad (2)$$

Electrophoresis. PAGE of purified proteins and complexes was carried out by using a Hoeffer minielectrophoresis system and the method of Schagger and Von Jagow (1987). Protein bands were stained with Coomassie Blue. Complexes for electrophoresis were made by adding enzyme and inhibitor (1:1.5, final concentration 2.5 μM) and incubating on ice for 2 h. Enzyme concentrations were determined from active site titration data, and α_2-antiplasmin concentration was determined by titration against plasmin. Complexes were dissociated by adding an equal volume of SDS sample buffer and heating to 100 °C for 15 min before loading 0.5 μg of protein/lane onto the gel.

Results

Lysine analogues are known to slow down complex formation between plasmin and α_2-antiplasmin in vitro [e.g., Wiman and Collen (1978)]. This is demonstrated in Figure 1, which shows binding curves for plasmin added to mixtures of α_2-antiplasmin and chromogenic substrate in the presence of a range of tranexamic acid concentrations. Clearly, for each curve there is a lag phase followed by a steady-state rate, and increasing tranexamic acid affects both the lag and the final rate. The steady-state rates are very low but are measurable over the long time periods used for these experiments. In control experiments (not shown) tranexamic acid was found to have no effect on plasmin hydrolysis of substrate (S-2251) at concentrations below 1 mM. Thus lysine analogues affect rate of reaction and the equilibrium position between enzyme and inhibitor. The same pattern is obtained in the absence of lysine analogues, but the lag is short and binding very tight, giving a K_i = 0.3 pM, calculated from known concentrations of proteins added and the amount of free enzyme remaining at equilibrium. This is a significant observation since previous mechanisms of serpin–serine protease binding have suggested the reaction was irreversible (Scheme I). This does not fit the experimental data as shown in Figure 2. Panel A shows the fit obtained if an irreversible reaction is assumed as outlined in the figure legend. Panel B shows the much improved fit using an equilibrium model. It can also been seen from Figures 1 and 2 that, following binding, there is no evidence of slow degradation of inhibitor.

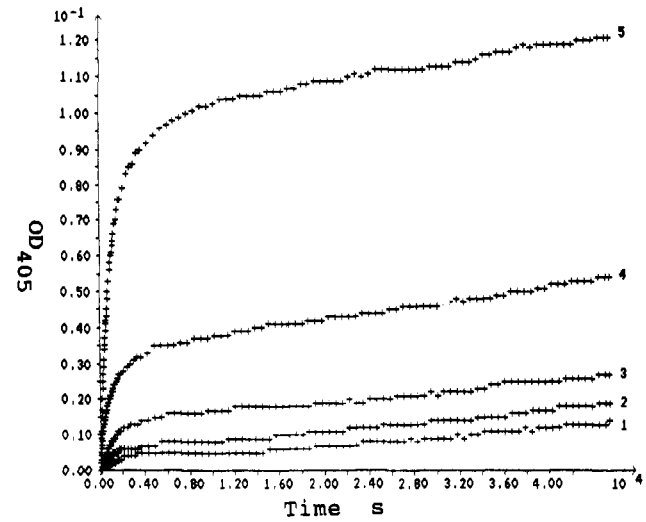

FIGURE 1: Binding of α_2-antiplasmin to plasmin in the presence of increasing concentrations of tranexamic acid. Plasmin (0.5 nM) was added to a solution containing chromogenic substrate (1 mM), α_2-antiplasmin (2.5 nM), and tranexamic acid at (1) 0 μM, (2) 10 μM, (3) 50 μM, (4) 100 μM, and (5) 500 μM. These experiments were performed in 0.1 M Tris-HCl buffer, pH 7.4, containing 0.01% Tween 80, at 25 °C.

Having established that the reaction involves an equilibrium between enzyme and inhibitor, it is necessary to determine whether binding is one step or two step as shown in Scheme II. It should be noted that reaction as far as complex formation is shown; while further processing to the cleaved inhibitor is not excluded, it will be very slow for a good inhibitor.

Scheme II

$$E + I \underset{k_{off}}{\overset{k_{on}}{\rightleftharpoons}} EI \qquad (A)$$

$$E + I \underset{k_{-1}}{\overset{k_1}{\rightleftharpoons}} EI \overset{\text{slow}}{\underset{k_{-2}}{\overset{k_2}{\rightleftharpoons}}} EI' \qquad (B)$$

$$E \overset{\text{slow}}{\underset{k_{-1}}{\overset{k_1}{\rightleftharpoons}}} E' + I \underset{k_{-2}}{\overset{k_2}{\rightleftharpoons}} EI' \qquad (C)$$

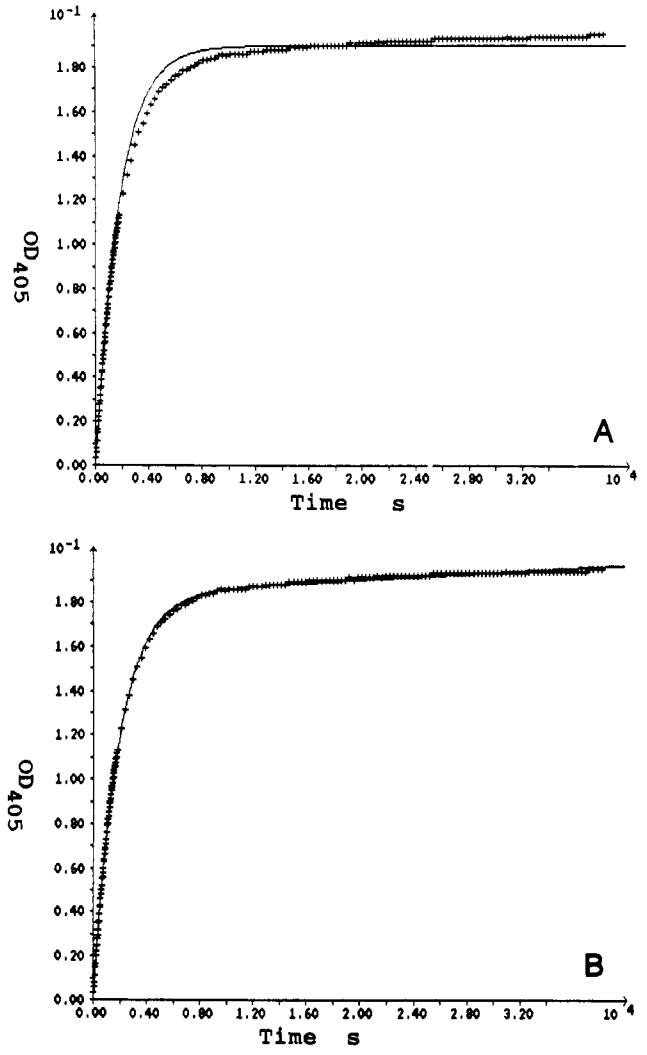

FIGURE 2: Typical binding of plasmin and α_2-antiplasmin with the data fitted to an irreversible and reversible reaction scheme. Panel A shows the fit using an irreversible model from the integrated rate equation $P = (1 - e^{A[I]t})V_m/A[I]$ [adapted from Tsou (1988)], where P = product concentration, $V_m = V_{max}$, A = apparent rate constant for binding, and [I] = inhibitor concentration. This fitting gave values for $k_1 = 7.3 \times 10^5$ M^{-1} s^{-1}, $k_{-1} = 2.3 \times 10^{-4}$ s^{-1}, and $k_2 = 2.5 \times 10^{-3}$ s^{-1}. However, the fit is poor because it ignores the final steady-state rate. Panel B shows data fitted well to eq 1 (Materials and Methods), the integrated rate equation for the reversible reaction under pseudo-first-order conditions as here.

By investigating inhibitor binding over a range of inhibitor concentrations, these three models can be distinguished [e.g., see Morrison and Walsh (1988)]. These experiments were performed in high concentrations of 6-aminohexanoic acid (15–50 mM), a second lysine analogue investigated, which can be seen to have similar action to tranexamic acid. In this way, inhibitor binding is slowed down and is easily monitored without rapid reaction equipment. Furthermore, the addition of lysine analogues will also mimic the situation in a clot where lysine groups are provided by fibrin. This is more interesting from a physiological viewpoint. When these experiments were performed and values determined for the variables in eq 1, we found v_0 to be inversely related to [I]. This disqualifies model A in Scheme II, according to which v_0 should be independent of inhibitor concentration. Model C can also be discounted because k' (eq 1) increases with increasing [I], which would not be the case with model C (Morrison & Walsh, 1988). Mechanism B is in agreement with the observed data. A plot of V_{max}/v_0 versus [I] can be used to calculate K_i, the initial dissociation constant for the loose complex in Scheme IIB.

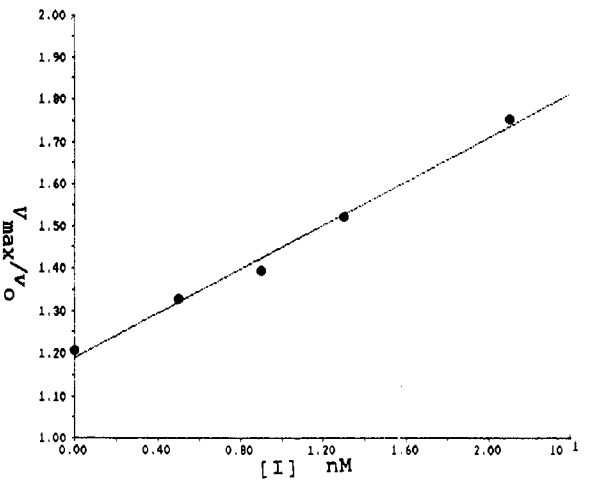

FIGURE 3: Plot for the determination of the K_i for the initial loose complex between plasmin and α_2-antiplasmin, in the presence of 50 mM 6-aminohexanoic acid. Values of v_0 were obtained from data fitted to eq 1 (Materials and Methods) over a range of inhibitor concentrations. K_i can be determined from the slope according to the equation $V_{max}/v_0 = K_m[I]/[S]K_i + (1 + K_m/[S])$ (Morrison & Walsh, 1988).

From the slope of this line, K_i is calculated to be 8 nM (Figure 3). Similarly, a plot of V_{max}/v_s versus [I] can be used to calculate K_i', the overall inhibition constant for the binding of plasmin and α_2-antiplasmin. This was calculated to be 2.4 ± 0.3 pM (mean ± SD, n = 3). Inhibition constants were calculated for interactions at 6-aminohexanoic acid concentrations above 15 mM. At lower concentrations, the data were not well fitted to eq 1. This possibly reflects equilibria between plasmin conformations. Values for K_i' were also calculated from plots of $(v_0 - v_s)/v_s$ versus [I] (data not shown), giving similar results. However, these inhibition constants are subject to some error since v_s is very low, and much smaller than v_0.

A value of k_{-2} the dissociation rate constant for the tight complex can be calculated from the relationship (Morrison, 1982):

$$k_{-2} = k'v_s/v_0 \quad (3)$$

This gives a value of $k_{-2} = (1.7 \pm 0.3) \times 10^{-6}$ s^{-1} (mean ± SD) by use of the variables fitted to eq 1. This corresponds to a half-life for the complex of 113 h (4.7 days), longer than the half-time of clearance from the plasma, which is 0.5 day (Collen & Wiman, 1979). Thus, even in the presence of fibrin, it is likely that complex formation is pseudoirreversible.

From these values, k_2 can be calculated from the relationship:

$$k_2 = [(K_i/K_i')(k_{-2})] - k_{-2} \quad (4)$$

This gives a value of $k_2 = 6 \times 10^{-3}$ s^{-1}.

k_2 can also be estimated from plots of k' versus [I], as shown in Figure 4. k' is well estimated from the data by using eq 1, not being significantly affected by low values of v_s. Estimates for k' have been fitted to a hyperbola (see Figure 4 legend), as required for mechanism B, Scheme II. However, it can be seen from Figure 4 that a straight line would also fit the data quite well over this range of inhibitor concentrations where mechanisms A and B in Scheme II cannot be distinguished from k' alone. The best fit of k_2 to the data generated from eq 1 gave $k_2 = (6.0 \pm 0.5) \times 10^{-3}$ s^{-1} (mean ± SD, n = 3). This agrees with the value calculated above. It is theoretically possible to derive a value for k_{-2} from the plots shown in Figure 4, from the intercept on the y axis. However, this is not valid when $k_{-2} \ll$ the values of k', and

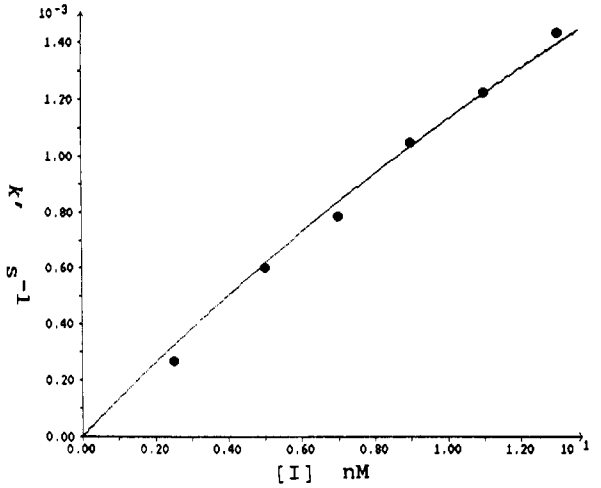

FIGURE 4: Dependence of k' on [I] for the determination of k_2 for the reaction of plasmin and α_2-antiplasmin in the presence of 50 mM 6-aminohexanoic acid. Values for k' were generated from data fitted to eq 1 (Materials and Methods) and the plotted data fitted to a hyperbolic curve by using the equation $k' = k_{-2} + k_2[([I]/K_i)/(1 + [S]/K_m + [I]/K_i)]$ (Morrison & Walsh, 1988).

Table I: Constants for the Binding of α_2-Antiplasmin to Plasmin and Chymotrypsin[a]

enzyme	K_i (k_{-1}/k_1) (nM)	K_i' (pM)	k_2 (s^{-1})	k_{-2} (s^{-1})
plasmin	8	2.4	0.006	1.7×10^{-6}
chymotrypsin	6.6	100	0.009	1.1×10^{-4}

[a] Reactions were performed at 25 °C in 0.1 M Tris-HCl, pH 7.4, containing 0.01% Tween 80 with plasmin; and in 0.144 M Tris-HCl, pH 7.74, containing 0.01% Tween 80 with chymotrypsin.

the intercept is very close to zero. The individual values for the various constants determined for plasmin–α_2-antiplasmin interaction at high 6-aminohexanoic acid concentrations (>15 mM) are shown in Table I.

Chymotrypsin is also known to be inhibited by α_2-antiplasmin, although less effectively than plasmin (Wiman, 1981). However, the mechanism of inhibition should be the same for both these serine proteases, so it is of interest to determine which rate constant(s) is(are) altered for the two interactions. Slow binding inhibition curves observed for the interaction of chymotrypsin with α_2-antiplasmin, as shown in Figure 5, were similar to those observed with plasmin, though they required a higher range of inhibitor concentrations due to the higher K_i' (up to 40 nM [I] gave suitable rates). Chymotrypsin was found to follow mechanism B in Scheme II, as demonstrated by the dependence of v_0 on [I], which was progressively reduced by 35% over the range of inhibitor concentrations shown in Figure 5. (See also Figure 6 for demonstration of mechanism B.) Analyzing the data as in Figure 3 above, by using V_{max}/v_0 or V_{max}/v_s versus [I], gave values of K_i = 6.5 nM and K_i' = 0.1 nM, respectively. Thus the inhibition constant for the formation of the initial loose complex is similar for both plasmin and chymotrypsin, but chymotrypsin goes on to form a less tightly bound complex. These values are likely to be more accurately determined for chymotrypsin because v_0/v_s is smaller than in the case of plasmin and α_2-antiplasmin. However, it should be stressed that α_2-antiplasmin is still a very potent inhibitor of chymotrypsin as demonstrated by the subnanomolar K_i'.

Figure 6 is a plot of $1/(k' - k_{-2})$ versus $1/[I]$, from which an estimate for k_2 can be derived (Shapiro & Riordan, 1984). Values for k_{-2} for the plot are determined by using the relationship shown in eq 3 above. The intercept on the y axis

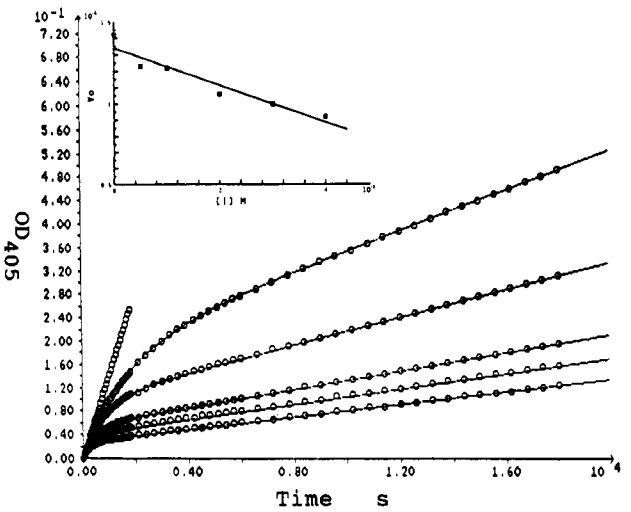

FIGURE 5: Slow binding inhibition kinetics for chymotrypsin and α_2-antiplasmin. Chymotrypsin (0.4 nM final concentration) was added to 0.5 mM chromogenic substrate and α_2-antiplasmin at concentrations of 0, 5, 10, 20, 30, and 40 nM, giving increasing levels of inhibition. All experiments were performed in 0.144 M Tris-HCl, pH 7.78, containing 0.01% Tween 80. The inset shows the decrease in initial rate, v_0, over this range of inhibitor concentrations.

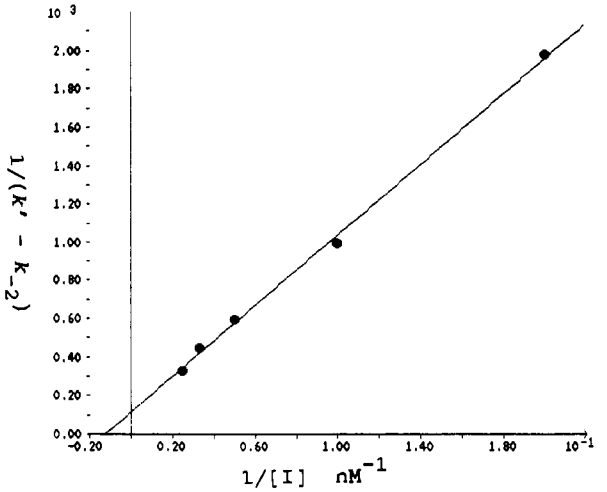

FIGURE 6: Determination of k_2 and K_i' for chymotrypsin and α_2-antiplasmin. To calculate $1/(k' - k_{-2})$, k_{-2} was determined according to eq 4. From the intercept on the y axis an accurate value of k_{-2} can be calculated. The intercept on the x axis is $-1/K_i'$(app). The plot does not pass through the origin, which is in accord with mechanism B, Scheme II [see Shapiro and Riordan (1984)].

provides a value of $k_2 = 9 \times 10^{-3}$ s^{-1}, and the intercept at $1/[I]$ is $-1/K_i$(app), giving a value of K_i = 6.6 nM, in very good agreement with the value calculated above from V_{max} and v_0. Figure 6 also demonstrates that mechanism B is in operation because the plot intercepts the y axis above zero, whereas for mechanism A the intercept would pass through the origin. From these values a more accurate value of k_{-2} can be calculated from the relationship in eq 4, to give $k_{-2} = 1.4 \times 10^{-4}$ s^{-1}.

In the case of chymotrypsin, k_{-2} is relatively high, and it should be possible to observe complex dissociation directly by diluting the complex into substrate ($t_{1/2}$ = 82.5 min, for a k_{-2} of 1.4×10^{-4} s^{-1}). This was done by forming approximately 1 μM complex on ice and diluting this to 0.25 nM in 0.9 mM substrate, such that $[EI] \ll K_i'$(app) [where K_i'(app) = $K_i'(1 + [S]/K_m)$]. In this way the equilibrium established between enzyme and inhibitor, which is apparent from Figure 5, is displaced by dilution and competing substrate toward free reactants E + I. When these experiments were performed,

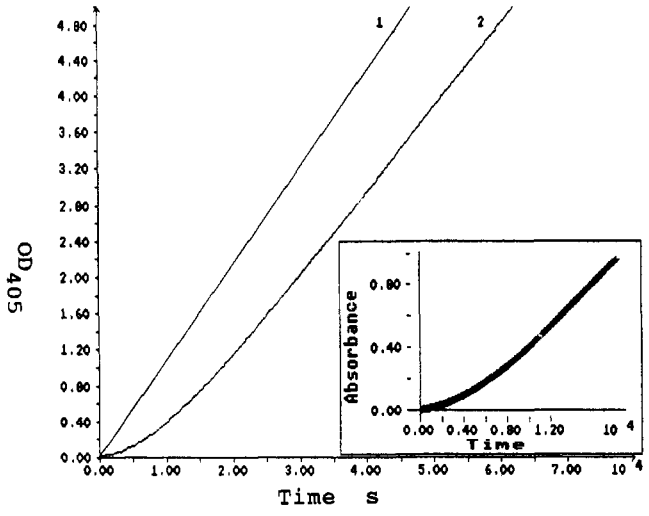

FIGURE 7: Dissociation of the chymotrypsin–α_2-antiplasmin complex by dilution into substrate. An aliquot of 1 μM complex was diluted (4×10^4)-fold into 0.9 mM chromogenic substrate, in 0.144 M Tris-HCl, pH 7.78, containing 0.01% Tween 80, at 25 °C. Dissociation was monitored by following free enzyme release and the hydrolysis of substrate (absorbance at 405 nm). Curve 1 is uninhibited enzyme, and curve 2 is the expected dissociation pattern from the results obtained and shown in the inset. A value for k_{-2} could be determined directly by fitting the data to eq 2 (Longstaff et al., 1990).

complex dissociation could indeed be observed as shown in Figure 7. When data from these experiments were fitted to eq 2, a value for this dissociation rate constant could be derived directly, which gave $k_{-2} = 1.1 \times 10^{-4}$ s^{-1}. This is in good agreement with the value calculated above. This would indicate the approaches used above for data analysis are valid. All the constants determined for the interaction of chymotrypsin and α_2-antiplasmin are shown in Table I.

Inhibition experiments with trypsin showed α_2-antiplasmin to be a very potent inhibitor of this enzyme in agreement with previous data (Wiman, 1981), but this interaction was difficult to study by the methods described above. α_2-Antiplasmin behaved as a simple competitive inhibitor of urokinase, with a K_i' of 42 nM, determined over a range of inhibitor concentrations from 0 to 75 nM.

Complexes formed between α_2-antiplasmin and the enzymes plasmin, chymotrypsin, trypsin, and urokinase were also studied by using SDS–PAGE. We find that dissociation and electrophoresis of these complexes produce a variable proportion of nondissociated complex, with the remainder dissociated and/or digested (not shown). The amount of dissociated complex is not related to inhibitory strength, and the pattern varies between experiments, suggesting dissociation/digestion is very sensitive to the conditions used.

Discussion

α_2-Antiplasmin was recognized some years ago, by several groups, as an extremely potent inhibitor of plasmin (Collen et al., 1976; Moroi & Aoki, 1976; Mullertz & Clemensen, 1976). Further work involving kinetic studies and observations of enzyme–inhibitor complexes in SDS–PAGE led to the proposal that the inhibitor acts by binding covalently and irreversibly to the serine protease (Scheme I). However, our kinetic analysis of binding has shown that this model may be oversimplified. We find a two-stage binding mechanism, involving two kinetically observable equilibria. Turnover of inhibitor is obviously very slow, and is not detected by our methods under these conditions. Having said this, our conclusions for the physiological situation would be the same as in earlier studies, since binding is so tight between plasmin and α_2-antiplasmin that complex formation can be considered to be pseudoirreversible. The fact that α_2-antiplasmin exists in equilibrium with plasmin does however have important implications for other systems, as discussed below.

In addition, some of our findings do not agree with other proposals for the action of α_2-antiplasmin. These are based on the observations shown in Figure 1 of binding curves with plasmin in the presence of a range of tranexamic acid concentrations. The same pattern is seen with 6-aminohexanoic acid. These curves show that increasing tranexamic acid slows down the binding of the inhibitor, as observed previously, but also affects the position of the final equilibrium. This argues that lysine analogues such as tranexamic acid do not act by blocking a second binding site for the inhibitor on the enzyme, but rather cause a conformational change in the enzyme. This type of conformational change is well documented for a variety of lysine analogues binding to plasmin or plasminogen [e.g., Brockway and Castellino (1972)]. This altered conformation is all that is needed to explain our observations on binding. Other workers have proposed two binding sites for the interaction between plasmin and α_2-antiplasmin following studies in which proteolytically modified plasmin was found to react more slowly (Wiman et al., 1978). It was suggested that the modified plasmin had lost the second binding site. However, caution must be exercised in drawing conclusions from modified proteins which are likely to have altered conformations. Overall, these results indicate that plasmin generated within a clot will have a zone of activity and exist for a finite time before it becomes inhibited. Binding is very tight (pseudoirreversible), and dissociation is very unlikely considering the physiological lifetime of the inhibited complex. The observed lifetime of the active enzyme will depend on the concentrations of plasmin, α_2-antiplasmin, and plasmin substrates.

The results of α_2-antiplasmin inhibition of chymotrypsin follow the same model proposed for inhibitor binding to plasmin and validate the approach used. Although chymotrypsin is not inhibited by α_2-antiplasmin physiologically, this is another tight binding serpin–serine protease interaction. Interestingly, α_2-antiplasmin is believed to bind to chymotrypsin using a different P_1 residue compared to the reaction with plasmin, such that the two reactive sites are not the same but do overlap (Potempa et al., 1988). However, it would be very surprising if a different mechanism was involved for binding of the two enzymes. Comparing the kinetics of the two reactions (Table I), it can be seen that the only significant difference is in the value of k_{-2}. Although this is the rate constant that has been ignored in all previous work (see Scheme I), it is common for inhibition strength to be determined by this rate constant [e.g., see Cha (1975)]. Dissociation rate constants are able to vary over a much wider range than association rate constants, which have a diffusion-controlled upper limit. This has been discussed elsewhere [e.g., see Fersht (1984)]. It should be stressed that the term "slow binding inhibition" does not require a low association rate but simply means a slow approach to equilibrium which is dependent on the association and dissociation rate constants [e.g., see Morrison and Walsh (1988)]. Thus it is not surprising to observe inhibitory strength determined by k_{-2}. However, this does have important consequences for serpin activity studies, as follows. In many cases where serpins bind very tightly to the serine protease, binding will appear to be pseudoirreversible, and dissociation can be ignored from a physiological standpoint. However, in some situations the equilibrium between enzyme and inhibitor may well be important, for example, when both proteins are present at very

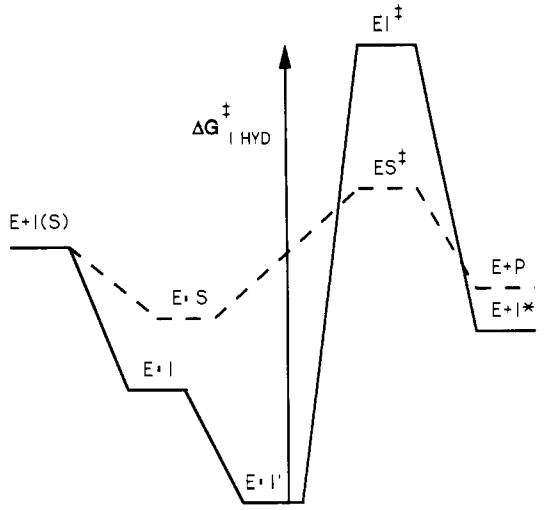

FIGURE 8: Proposed reaction profile for serpin inhibition of serine proteases following the reaction $E + I \rightleftharpoons EI \rightleftharpoons EI' \rightarrow E + I^*$. Inhibition is caused in two ways. (i) The large barrier to hydrolysis resulting from the low energy of EI′ (the enzyme–inhibitor complex, resembling the Michaelis complex in enzyme substrate reactions; see dashed line). This is by virtue of a high degree of enzyme–substrate complementarity. (ii) The high energy of the transition state EI* resulting from inherent inhibitor strain resisting deformation to the tetrahedral transition state. The complex is thus in a "thermodynamic pit" ($\Delta G^{\ddagger}_{I\,HYD}$ is large), making formation of I* highly unfavorable, as expected for a good inhibitor.

low concentrations ($[E_0] \approx [I_0] \leq K_i'$). This may well be the case for the interaction of t-PA and PAI-1, for example, in vivo and during in vitro assays. In addition, with systems involving serpins that inhibit less potently, or with mutant proteins, a significant portion of enzyme activity may remain at equilibrium, unless a large excess of inhibitor is present. In any event, inhibitory strength is best expressed as K_i', i.e., the overall inhibition constant for the system, rather than as an association rate constant, as is common practice.

Mechanism of Serpin Action. Early work on the crystal structure of trypsin and BPTI led to the conclusion that complexes were covalently bound, with the normal cleavage reaction arrested close to the tetrahedral transition state (Rühlmann et al., 1973). By analogy with this, and from the kinetic data leading to the mechanism shown in Scheme I, it was proposed that α_2-antiplasmin reaction with plasmin led to the same complex (Wiman & Collen, 1979). This mechanism of binding has also been proposed for other serpins (Travis & Salvesen, 1983). However, later, highly refined crystal structures of protein inhibitors like BPTI (Kunitz inhibitors, ovomucoid inhibitors, etc.) have led to the conclusion that, when bound to serine proteases, the structures are close to a Michaelis complex and no covalent bond exists between the two proteins (Read & James, 1986). This is supported by NMR data (Richarz et al., 1980; Baillargeon et al., 1980). However, so far there is no crystal structure of an intact serpin, or a serpin complex. On the basis of the results presented here we would suggest that the kinetics of serpin binding are very similar to those for other protease inhibitors of the type mentioned above (Laskowski & Kato, 1980) and the mechanism of inhibition may well be the same. This would support the notion that serpins and serine proteases are not covalently bound. There is no reason why a covalent bond is necessary to explain inhibitory strength, and we would suggest that there is no real evidence for it. One technique often used to support the notion that the complex is covalently bound is SDS-PAGE. As we stated under Results, we find the amount of complex observed on gels is variable and bands corresponding to free enzyme and inhibitor, and to various degradation products, are always significant. This is also seen in many gels published in the literature. We feel that SDS treatment leads to some covalent bond formation and other artifacts. Thus we would propose that serpins can inhibit serine proteases by the same mechanism that other small proteins do, which may be explained by Figure 8. This has been discussed elsewhere with reference to the small protease inhibitor, chymotrypsin inhibitor 2 (Longstaff et al., 1990). However, one notable difference between serpins and other small protein inhibitors is that cleaved serpins are inactive due to their altered conformation [e.g., Carrell and Boswell (1986)], unlike other families of inhibitors in which cleaved inhibitors remain active (Laskowski & Kato, 1980). This is not important to the proposed mechanism outlined in Figure 8. Serpins bind via an active site loop, to form a 1:1 complex, where the two steps observed in complex formation represent docking of the two partners. The loop is complementary to the active site cleft of the protease, resulting in an enzyme–inhibitor complex with a very low energy compared to a normal substrate. A further barrier to hydrolysis is the strain in the serpin molecule, which may act to raise the energy of the tetrahedral transition state. Serpins are known to be highly strained from data from a number of physical techniques [e.g., see Carrell and Boswell (1986)], and furthermore, molecules such as ovalbumin, which are members of this superfamily but which do not have the strained to relaxed conformational change, have no inhibitory activity. These ideas are proposed as a basis for future work, but the structure of the inhibited complex and mechanism of action will only be settled when a high-resolution crystal structure becomes available.

ACKNOWLEDGMENTS

We thank Dr. H. R. Lijnen for the α_2-antiplasmin. We thank Professor A. A. Sasahara (Abbott Laboratories) for the gift of plasminogen. We are grateful to Wakomoto Laboratories and Serono Laboratories for providing urokinase. We thank Professor R. W. Carrell for helpful discussions.

Registry No. Serine protease, 37259-58-8; chymotrypsin, 9004-07-3; plasmin, 9001-90-5; serpin, 96282-35-8.

REFERENCES

Baillargeon, M. W., Laskowski, M., Jr., Neves, D. E., Porubcan, M. A., Santini, R. E., & Marklay, J. L. (1980) *Biochemistry 19*, 5703–5710.

Brockway, W. J., & Castellino, F. J. (1972) *Arch. Biochem. Biophys. 151*, 194–199.

Carrell, R. W., & Boswell, D. R. (1986) in *Proteinase Inhibitors* (Barrett, A. J., & Salvesen, G., Eds.) pp 403–420, Elsevier, Amsterdam.

Cha, S. (1975) *Biochem. Pharmacol. 24*, 2177–2186. Collen, D., De Cock, F., & Edy, J. (1976) *Eur. J. Biochem. 69*, 209–216.

Collen, D., & Wiman, B. (1979) *Blood 53*, 313–324.

Deutch, D. G., & Mertz, E. T. (1970) *Science 170*, 1095–1096.

Fersht, A. R. (1984) in *Enzyme Structure and Mechanism*, 2nd ed., Freeman, New York.

Huber, R., & Carrell, R. W. (1989) *Biochemistry 28*, 8951–8966.

Jameson, G. W., Roberts, D. V., Adams, R. W. A., Kyle, W. S. A., & Elmore, D. J. (1973) *Biochem. J. 131*, 107–117.

Laskowski, M., Jr., & Kato, I. (1980) *Annu. Rev. Biochem. 49*, 593–626.

Leatherbarrow, R. J. (1987) *Enzfitter, a program for nonlinear regression analysis*, Elsevier Scientific, New York.

Lijnen, H. R., van Hoef, B., & Collen, D. (1981) *Eur. J. Biochem. 120*, 149-154.
Longstaff, C., Campbell, A. F., & Fersht, A. R. (1990) *Biochemistry 29*, 7339-7347.
Moroi, M., & Aoki, N. (1976) *J. Biol. Chem. 251*, 5956-5965.
Morrison, J. F. (1982) *Trends Biochem. Sci. 7*, 102-105.
Morrison, J. F., & Walsh, C. T. (1988) *Adv. Enzymol. 61*, 201-301.
Mullertz, S., & Clemmensen, I. (1976) *Biochem. J. 159*, 545-553.
Nieuwenhuizen, W., & Traas, D. W. (1989) *Thromb. Haemostasis 61*, 208-210.
Ohlsson, K., & Laurell, C.-B. (1976) *Clin. Sci. Mol. Med. 51*, 87-92.
Potempa, J., Shieh, B.-H., & Travis, J. (1988) *Science 241*, 699-700.
Read, R. J., & James, M. N. G. (1986) in *Proteinase Inhibitors* (Barret, A. J., & Salvesen, G., Eds.) pp 301-336, Elsevier, Amsterdam.
Richarz, R., Tschesche, H., & Wurtrich, K. (1980) *Biochemistry 19*, 5711-5715.
Rühlhman, A., Kukla, D., Schwagen, P., Bartels, K., & Huber, R. (1973) *J. Mol. Biol. 77*, 417-436.
Schägger, H., & Von Jagow, G. (1987) *Anal. Biochem. 166*, 368-379.
Schechter, I., & Berger, A. (1967) *Biochem. Biophys. Res. Commun. 27*, 157-162.
Shapiro, R., & Riordan, J. F. (1984) *Biochemistry 23*, 5234-5240.
Shieh, B.-H., Potempa, J., & Travis, J. (1989) *J. Biol. Chem. 264*, 13420-13423.
Travis, J., & Salvesen, G. S. (1983) *Annu. Rev. Biochem. 52*, 655-709.
Tsou, C. L. (1988) *Adv. Enzymol. 61*, 381-436.
Wiman, B. (1981) *Methods Enzymol. 80*, 395-408.
Wiman, B., & Collen, D. (1978) *Eur. J. Biochem. 84*, 573-578.
Wiman, B., & Collen, D. (1979) *J. Biol. Chem. 254*, 9291-9297.
Wiman, B., Boman, L., & Collen, D. (1978) *Eur. J. Biochem. 87*, 143-146.

Analysis of ϕ and χ_1 Torsion Angles for Hen Lysozyme in Solution from ^{1}H NMR Spin-Spin Coupling Constants†

Lorna J. Smith, Michael J. Sutcliffe,‡ Christina Redfield, and Christopher M. Dobson*
Oxford Centre for Molecular Sciences and Inorganic Chemistry Laboratory, University of Oxford, South Parks Road, Oxford OX1 3QR, England

Received July 30, 1990; Revised Manuscript Received October 8, 1990

ABSTRACT: Three-bond $^3J_{HN\alpha}$ coupling constants have been determined for 106 residues and $^3J_{\alpha\beta}$ coupling constants have been measured for 57 residues of the 129-residue protein hen egg white lysozyme. These NMR data have been compared with torsion angles defined in the tetragonal and the triclinic crystal forms of the protein. For most residues the measured $^3J_{HN\alpha}$ values were consistent with the ϕ torsion angles found in both crystal forms; the RMS difference between the coupling constants calculated by using the tetragonal crystal structure ϕ angles and the experimental $^3J_{HN\alpha}$ values is 0.88 Hz. Thus there appears to be no significant averaging of the ϕ torsion angle either in the interior or at the surface of the protein. For 41 of the residues where $^3J_{\alpha\beta}$ coupling constants have been determined, the values are consistent with a single staggered conformation about the χ_1 torsion angle and there is complete agreement between the NMR data in solution and the torsion angles defined in the crystalline state. In contrast, for the other 16 residues where $^3J_{\alpha\beta}$ coupling constant values have been measured, the data indicate extensive motional averaging about the χ_1 torsion angle. These residues occur largely on the surface of the protein and examination of the crystal structures shows that many of these residues adopt a different conformation in the triclinic and tetragonal crystal forms and have high crystallographic temperature factors. It appears, however, that in solution conformational flexibility of the side chains of surface residues is significantly more pronounced than in individual crystal structures.

Developments in NMR[1] spectroscopy in recent years have made it possible to begin systematic comparisons between the structures and dynamic properties of proteins in solution and crystalline states (Clore & Gronenborn, 1987; Billeter et al., 1989). The study of the main-chain conformations of proteins is particularly favorable both by crystallographic techniques and by NMR spectroscopy. In the case of X-ray crystallography, the continuous density associated with the polypeptide chain enables it to be traced through the electron density map provided that the map is of sufficiently high resolution (Blundell & Johnson, 1976). From NMR spectroscopy, nu-

† This work was supported by the U.K. Science and Engineering Research Council.
* To whom correspondence should be addressed.
‡ Present address: Biological NMR Centre, Medical Sciences Building, Leicester University, University Road, Leicester LE1 9HN, U.K.

[1] Abbreviations: NMR, nuclear magnetic resonance; NOE, nuclear Overhauser enhancement; COSY, two-dimensional *J*-correlated spectroscopy; DQF COSY, two-dimensional double quantum filtered correlation spectroscopy; E. COSY, two-dimensional exclusive correlation spectroscopy; NOESY, two-dimensional nuclear Overhauser enhancement spectroscopy; RMS, root mean square.

0006-2960/91/0430-986$02.50/0